Evaluation and Advancement of Histological Imaging Modalities for Osteoarthritis Applications

Margaret "Meggie" Pires-Fernandes

Supervisory Committee:

Dr. Kyle Allen
Dr. Blanka Sharma
Dr. Heather Vincent

Oral Defense Date
April 6, 2018

Abstract

Osteoarthritis (OA) is a disease that impacts the entirety of an affected articular joint. OA is most commonly studied in preclinical animal models. One key aspect of studying the disease is analyzing the microscopic changes that occur in the joint space. Histology is the study of microscopic structures of tissues, and there exists histological grading schemes to quantify the changes that occur in response to disease or injury.

Two methods specifically, the Pritzker and Gerwin, were evaluated and compared across two models of OA: the MIA, a chemical model, and the MMT, a surgical model. No differences in grading were present between the MIA and MMT model when the Pritzker scheme was used. Differences between the two models were present in tibial plateau length, osteophyte size, and zone 3 (lateral) cartilage degeneration scores in the Gerwin scheme.

Histology provides valuable metrics about the progression of OA, but there are imaging methods that can be adapted for OA research. With confocal microscopy and porcine meniscus, immunohistochemical staining and clearing protocols were combined to allow for optical sectioning through the tissue. From this study, it was determined that clearing the samples twice increased the imaging depth of the tissue.

In the final piece of this work, the staining and clearing protocols were adapted to whole mouse joints, and were imaged on a selective plane illumination microscope (SPIM). From this work, it is clear that SPIM provides advantages over confocal imaging and has the potential to provide information about how the entire joint changes as a result of OA via facilitating 3D histological analysis of whole joints.

Introduction

Osteoarthritis (OA) is a complex disease of the articular joint that leads to pain and disability. Clinically, knee OA is the most prevalent form of the disease among people aged 65 and older, and is the leading cause of disability in the US [1]. There is currently no treatment that undoes the structural damage caused by the progression of the disease, and most care focuses on reducing OA-related pain and increasing functionality for the patient [2]. This symptom-reducing care imposes a burden on the American health care system, and in 2010 healthcare expenses were $46.6 billion [3]. If researchers and clinicians can better understand the underlying mechanisms of the disease and successfully develop disease-altering treatment options for patients, both the patients and the healthcare system will be benefited. OA is studied in both clinical and preclinical studies. However, clinical studies are limited by variations in the onset of symptoms and prognosis of the disease, which can make it challenging to accurately study the disease [4]. In contrast, preclinical studies can be utilized to accurately track the progression of the disease and evaluate treatment modalities in a systematic and highly controlled manner [5]. Preclinical animal studies are useful for understanding the pathogenesis of OA and evaluating the efficacy of treatments [5]. For preclinical animal studies of OA, particularly in rodents, utilization of chemically and surgically induced models of the disease is common.

Although these models are not perfect analogues of the clinical condition, they can provide similar morphological changes that resemble those occurring in some stages of OA [6]. The morphological changes that occur as a result of these induced models of OA provide valuable information about disease progression. The changes that occur in the joint space are typically characterized by cartilage degradation, bone remodeling, osteophyte formation, and inflammation [7]. The four components of the synovial joint that are impacted by OA are the meniscus, articular cartilage, subchondral bone, and synovial membrane [8].

These morphological changes are most commonly studied via histology: the study of the microscopic structures of tissues. There are a variety of methods to stage, grade, and characterize histological data. Because validation, evaluation, and quantification of OA-model joint related degradation is critical to understanding the underlying mechanisms of the disease, it is important

to identify and evaluate difficulties and discrepancies in traditional methods of histological grading, and improve pre-existing methods of histopathology.

Shown below is the logical flow of this work, in which traditional methods of histology grading will be described and compared, and suggestions will be made on how to better standardize these practices in the field of rodent models of osteoarthritis. Then, methods to better utilize and image samples will be described, as well as the progress made thus far in that direction.

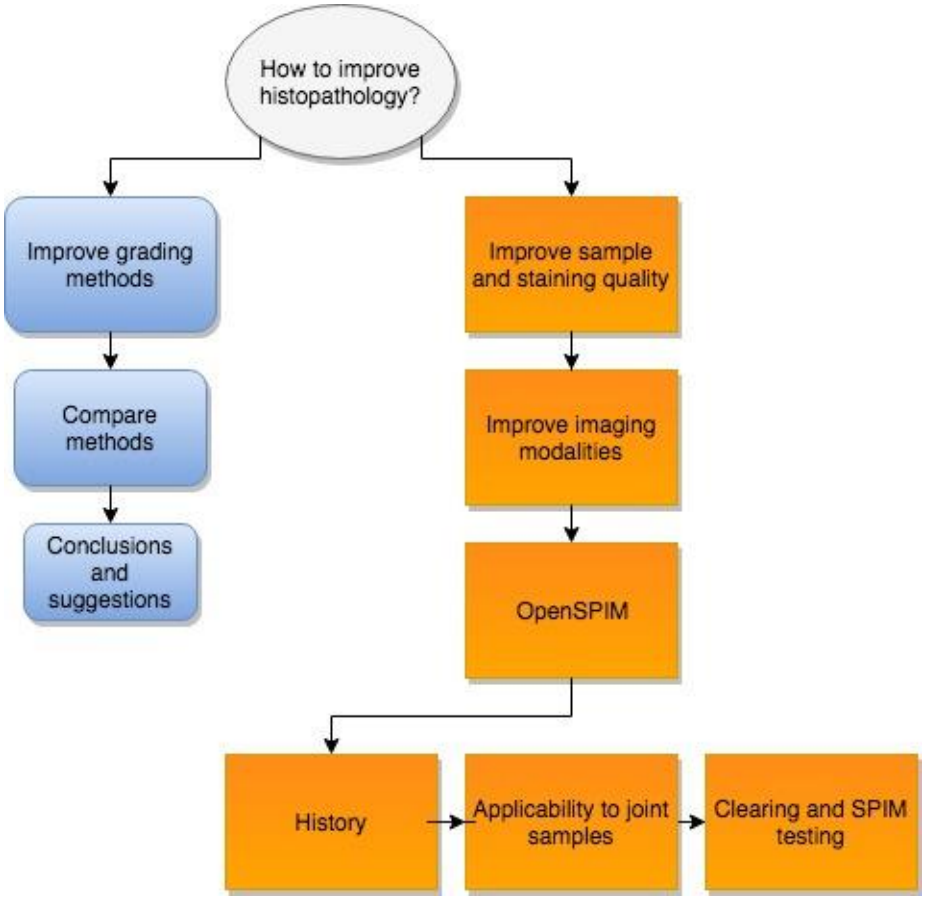

Figure 1. Flowchart depicting the logical flow of the work completed in this thesis.

Traditional Methods of OA Histopathology Evaluation

Histopathology is the historical method of assessing OA measures of degeneration and is currently the accepted gold standard [9]. Two methods of histological grading for OA models have been described by Pritzker *et al*, and Gerwin *et al* [10], [11], [12]. These two methods of evaluating histological images aim to quantify the physical anatomical changes that occur in the joint space.

The 2006 Pritzker scheme aims to leverage five valuable principles: simplicity, utility, scalability, extendibility, and comparability [10]. The Pritzker scheme uses a combination of grades and stages to evaluate the depth of lesions and extent of OA progression on the joint surface [10]. Grade relates to the depth of the progression of lesions into the cartilage and stage relates to the extent of OA on the surface of the cartilage [10]. The overall score is defined as the combined OA grade and OA stage and yields valuable information about the severity and extent of OA in the joint [10]. The grades signify the depth of progression into the cartilage and progress from Grade 0 to Grade 6; Grade 0 relates to an intact surface and cartilage morphology, while Grade 6 relates to deformation including bone remodeling [10]. The levels of degradation that relate to grades progress as follows: surface and cartilage morphology intact, surface intact, surface discontinuity, vertical fissures (clefts), erosion, denudation, and deformation [10]. The OA stage is representative of the proportion of the articular surface that is affected by OA compared to the total surface length, regardless of the OA grade or if lesions are discontinuous [10]. There are four stages that signify the horizontal extent of the cartilage surface that is degraded and the percentage of surface, area, and volume of the cartilage that is involved in the degeneration is measured [8]. Stage 0 represents no OA present, Stage 1 is less than 10% involved, Stage 2 is 10-25% involved, Stage 3 is >50% involved, and Stage 4 is >50% involved [10]. The total score is calculated by multiplying the stage number and grade number [10].

The 2010 Gerwin Scheme similarly aims to quantify the state of OA in rodent models, but has the specific goal of providing utility across different rodent models of OA and across researcher groups [11]. It utilizes three sections representative of the "most damage" in a joint sample and requires specific measurements for a variety of locations in the joint space. The method of grading is based on measurements for 10 predefined parameters [11]. These parameters are cartilage matrix loss width, cartilage degeneration score, total cartilage degeneration width, significant cartilage

degeneration width, zonal depth ratio of lesions, osteophytes, calcified cartilage and subchondral bone damage score, synovial reaction, medial joint capsule repair, and growth plate thickness [11]. It is recommended that three sections per joint are analyzed and the mean and standard error for each parameter or measurement is calculated for the total score [11]. Gerwin suggests that although this method of evaluating the joint is more complex than other grading methods, that it is easily understood, reproducible, and suitable for novice graders [11].

Multiple rodent models of OA elicit different features of OA related to clinical presentations of the disease. The most commonly used methods to induce OA related changes can be considered either chemical or surgical models. Both chemical and surgical models provide valuable information to the study of the disease, however the differences in the pathogenesis of these models cause challenges in the comparison of results [6]. Surgically induced models, like the medial meniscal transection (MMT), allow for high reproducibility and short-term studies due to rapid progression of the disease [6]. These models often produce pathologic changes similar to post-traumatic OA in human patients. Chemically induced models, like the monoiodoacetate (MIA) injection model, do not progress in a way that parallels clinical OA, but also develop quickly and are often used to study the mechanisms associated with OA pain [6]. The MMT and MIA models also vary in the rate and extent of joint damage seen over time [6].

Because these models differ in their effects on the joint and histological evaluation methods differ in comprehensiveness, identifying grading methods that accurately represent the state of the joint and type of damage associated with each model is an important consideration. In this section, the Pritzker and Gerwin evaluation methods were compared across the rodent MIA and MMT models. This was done by comparing the individual parameters outlined by both the Pritzker and Gerwin methods within the two models.

Evaluation of Traditional Methods of OA Histopathology

Methods

Male Lewis rats received either the MMT (n=5) surgery or an intra-articular injection of MIA (n=8) in the right knee. Four weeks post-op, the rats were euthanized and both ipsilateral and contralateral knees were collected for histology. Ten micrometer frontal slices were collected through the central region of the joint. The central region is defined as the sections past the anterior horn of the medial meniscus through the posterior horn of the meniscus. The sections were then stained with a 1% Toluidine Blue solution. All slides from the loading zone of the joint were analyzed and the slides representing the worst damage were graded using both the 2006 OARSI method described by Pritzker et al and the 2010 OARSI method described by Gerwin et al. Statistical analysis was completed by performing a two-tailed student's t-test as well as the F-test with a significance determined at $p < 0.05$.

Results

With the Gerwin grading scheme, tibial plateau length ($p < 0.0004$), osteophyte size ($p < 0.02$), zone 2 (central) ($p < 0.006$), and zone 3 (lateral) ($p < 0.005$) cartilage degeneration scores were significantly different between the MIA and MMT groups as indicated by a two tailed t-test (Figure 2). The differences seen between the groups specifically concerning cartilage features may be due to MIA joints often completely missing the components necessary for scoring. The variability in cartilage degeneration scoring in the lateral third of the medial compartment was significantly greater in the MIA model than the MMT model as indicated by an F-test. Under the Pritzker scheme, there were no significant differences found between models in either grade or stage. However, the MIA model showed significant variability in scoring as compared to the MMT model as indicated by an F-test. Shown below in Figure 3 are representative histology slides from the MIA, MMT and naïve groups. It is clear that there are stark structural differences between the MIA and MMT groups.

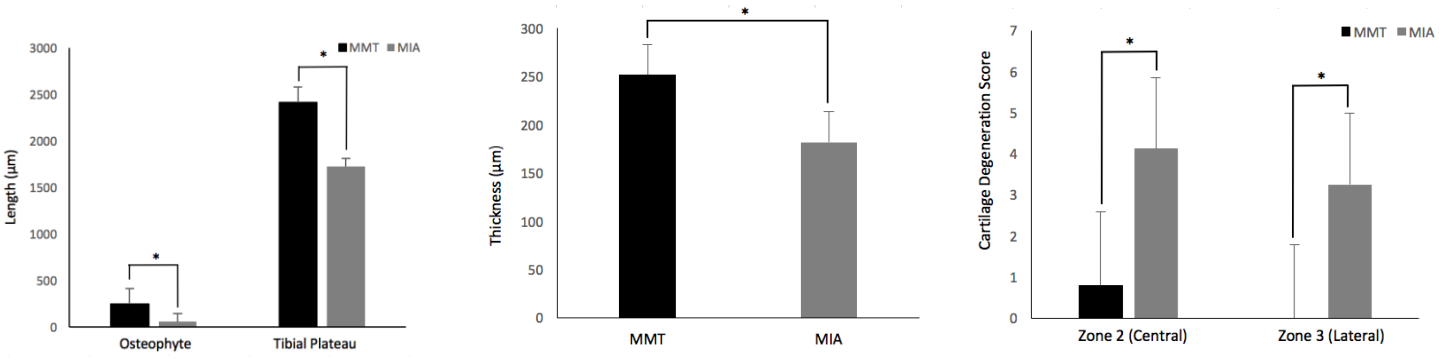

2A 2B 2C

Figure 2. Differences between MIA and MMT models in measurements of parameters defined by the Gerwin scheme. 2A shows the differences between the models in zone 2 (central) and zone 3 (lateral). 2B show the differences in medial growth plate thickness between the two models. 2C show the differences in sizes of tibial plateaus and osteophytes.

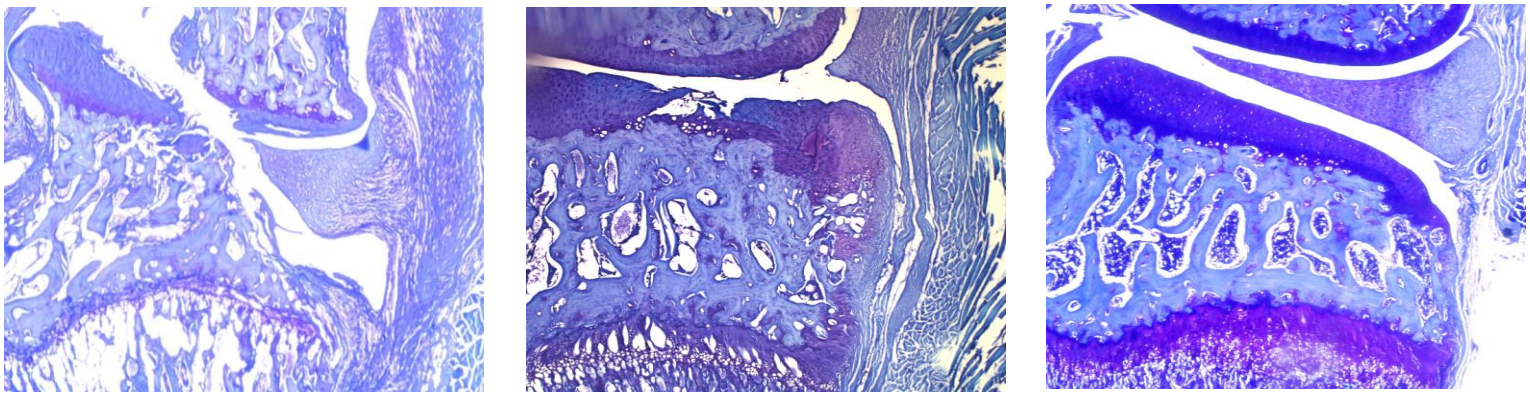

3A 3B 3C

Figure 3. Representative histology slides from the MIA (3A), MMT (3B), and naïve (3C) groups.

Discussion

The Pritzker and Gerwin grading schemes were chosen for their widespread use and focus on assessing cartilage degeneration, an important assessment of OA severity [6]. The Pritzker score assigns a single semi-quantitative rank to the histological image. This aspect of the Pritzker grading scheme serves to be advantageous to quickly assess mild degeneration. Additionally, this scheme may be applied more consistently by novice users because of the overall simplicity of the method of grading. The simplicity of the method can also lead to more consistency in grading because there are fewer options to choose from within the grades and stages. A limitation of this grading scheme, however, is that only the depth and width of the cartilage degeneration is accounted for, rather than evaluating multiple OA features. The Gerwin scheme is more detailed, and is also specific to rats, providing physical measurement of both cartilage degeneration and bony changes.

For models that exhibit focal lesions and osteophyte growth, like the MMT model, the Gerwin scheme is more descriptive. However, for models where the whole joint surface is affected, like the MIA model, this may cause the overall joint score to be misrepresented. For example, the osteophyte size for the MIA model was significantly lower than the osteophyte size for the MMT model, but this is likely due to that area of the joint having significant structural degeneration. This would contribute to an overall lower degradation score in the Gerwin model, and potentially interpreted as having a decreased degeneration score when that may not be an accurate representation. This lack of accuracy may also be due to the pathogenesis seen in the MIA model, where classic OA features like osteophytes are rarely present, and some areas in the joint are not gradable due to widespread cell death. Therefore, certain measures in the Gerwin scheme may not accurately represent damage seen across the MIA and MMT models and cause joint degeneration scores to be inaccurately represented. Finally, the Pritzker scheme is useful due to its relatively simple design, however it may not be the most robust method of quantifying degeneration in OA models. The Gerwin scheme incorporates more affected areas of the joint space, however may not be as translatable to models, like the MIA model, that cause structural deformations.

Overall, when selecting a grading scheme for the histological assessment of a knee OA model, it is important to consider the specific damage and degeneration associated with the progression of that model. Chemical and surgical models of OA progress differently and are characterized by

different features. Selecting a grading scheme that is highly repeatable and accounts for the appropriate features for the selected model can improve the utility and accuracy of histological grading. Additionally, OA is a disease of the entire joint, however, and these two grading schemes are limited when attempting to identify joint features beyond those in bone and cartilage that may contribute to the assessment of overall joint degeneration. Quantifying the degeneration of the joint as a whole, including measures beyond cartilage and bony changes alone, may give better insight into the overall mechanisms of disease progression [11].

Traditional histopathology practices and methods of assessing results have associated variability. Poor fixation, dehydration, and sectioning can impact the integrity of the tissues and physical sectioning and staining can introduce artefacts into the samples contributing to existing variability [12]. The mechanical stresses of sectioning the tissues may cause pieces of sample to be lost, and the process of deparaffinization may cause chemical damage [12]. These factors may also impact the way tissue is graded with both the Gerwin and Pritzker methods. In this respect, advancing histological sample preparation, collection, and imaging methods may assist in improving the accuracy of histological grading with either of these, or other, grading methods.

Methods for Advancing the Study of OA

The traditional methods of histopathology are by no means obsolete, but there are advanced methods of imaging that may augment analysis of the joint space. Such methods, like confocal microscopy and selective plane imaging microscopy, will be evaluated for this purpose.

Confocal microscopy is a modern imaging modality that has many advantages over traditional bright field microscopy. Confocal microscopy utilizes laser scanning to optically section a sample and produces high resolution 3D reconstructions. One advantage is that optical sectioning does not induce physical alterations to the tissue as with traditional histology, due to chemical processing and mechanical slicing [13]. As mentioned, there can be negative impacts on the quality of the histology slices, like tissue shrinking or loss of tissue [12,13]. Confocal microscopy also utilizes fluorescence to track specifically stained structures or regions of a sample [13]. Confocal imaging and fluorescent staining of specific biological membranes can be applied to the study of

osteoarthritis and allow for more specific tracking of changes in the joint space. This is particularly useful in OA research, as OA leads to changes throughout the entire joint. Having data on the overall changes that occur in the joint space, not just degraded articular cartilage, osteophyte formation, or other typical cartilage and boney changes, may give greater insight into how the joint changes with disease progression. Additionally, the utility of a single sample is increased with confocal imaging techniques, because one sample can potentially be stained multiple times with dyes that are excited and emit at different wavelengths, allowing a collection of features to be tracked within a single sample. Confocal settings can usually be changed to excite certain wavelengths that are captured simultaneously as separate images, and post processing can overlay the images to see the overall result.

In order to use confocal microscopy or SPIM, samples must be optically clear. This is due to the nature of the imaging technique, which requires that light pass through the tissue [14]. Light scattering occurs when there is heterogeneity in the amount of scattering in different areas of a tissue, but is often described as being due to a mismatch of refractive indices at the tissue interfaces [14]. When this happens, it is perceived as opaqueness in the tissue. Tissue clearing methods are not meant to prevent light scattering, but are supposed to create a high uniform density of scatters to allow the light to pass through the tissue [14]. The more optically clear the tissue, the more heterogeneity in the light scattering and the more opaque the tissue will be. Simply put, light scatter is a phenomenon encountered in imaging due to mismatches in the refractive index of the materials through which light passes, leading to overall loss of signal, reduced imaging depth, and decreased image quality[15], [16].

Immersion based optical clearing utilizes refractive index matching between sample tissues and a clearing media. The combination of SPIM and optical clearing may prove to be a valuable enhancement in whole sample imaging and providing more data from each sample with better image quality. Augmenting 2D histological data in OA models with immunohistochemical stains and 3D sample reconstruction will allow for better assessment of whole joint changes with these methods. In this study, the combination protocol of a fluorescent immunohistochemical staining protocol and recommended clearing protocol for orthopedic tissue was developed and validated

using a confocal microscope, with the intent of future application of this sample preparation for SPIM.

Methods

Frozen porcine menisci were obtained from Animal Technologies (Tyler, Texas). Three pairs of menisci were thawed and 4 mm plugs were taken from the lateral and medial sides of each meniscus. Three plugs were taken from both the lateral and medial sides and distributed evenly into three groups (n=18). Berke *et al* previously published work evaluating multiple aqueous and non-aqueous optical clearing solutions [17]. Their results indicated that methyl salicylate, a non-aqueous solution, provided a greater level of clearing for musculoskeletal samples (which typically have a high refractive index relative to other tissues commonly processed with optical clearing methods) than other solutions without being highly toxic or expensive [17]. The protocol begins with sample dehydration via graded ethanol baths until the samples are in 100% ethanol [17]. The samples are then immersed in 2-propanol, and finally immersed in the optical refractive index matching solution, methyl salicylate [17]. The samples cleared within 24 hours and fresh methyl salicylate was added before imaging.

The menisci were stained in two different solutions to stain both cells and the extracellular matrix (ECM). The stains were selected based upon previous work by Upton *et al* [18]. The samples were washed twice in D-PBS for 3 min and then incubated in freshly diluted fluorescent dyes. The cells were stained for with SYTO64 (2 micro molar final concentration in D-PBS, 90 min, 37 ℃) and the ECM was stained for with dichlorotriazinlyamino fluorescin (DTAF) (2 mg/mL in 0.2 M sodium bicarbonate buffer pH 9.0, 15 min, room temperature) [18]. These stains were chosen due to their ability to show generalized features of the tissue [18]. Meniscus samples were protected from light due photosensitivity of the dyes. The three groups of menisci (total n=18) were tested using different staining and clearing orders to identify the most appropriate sequence of incorporating the two protocols. The first group was stained and uncleared (UC), the second groups was stained and then cleared (C1), and the third group was cleared, stained, and then re-cleared (C2). The third group was re-cleared due to the aqueous nature of the dye and non-aqueous nature of the clearing agent, requiring that samples be re-cleared after exposure to the aqueous dye.

The menisci samples were imaged on a Leica TCS SP5 confocal laser scanning microscope and optical sections were captured every 5 microns. The imaging depth was calculated by identifying where in the sample the middle section was no longer visible using ImageJ. Statistical analysis was completed by performing a two-tailed student's t-test with $p < 0.05$ considered significant.

Results

The average imaging depth for the UC, C1, and C2 groups were 116.7, 185, and 217.5 microns with standard deviations 40.1, 20.2, and 24.08 microns, respectively. The three groups had significant differences in their average clearing depth into the tissue, with $p < 0.006$ between uncleared and cleared once, $p < 0.0008$ between uncleared and cleared twice, and $p < 0.03$ between cleared once and cleared twice. The green colored section is the area of the sample stained with DTAF to visualize the ECM and the red colored sections are the areas of the sample stained with SYTO64 for cell visualization. Images of a representative sample at 75 microns into the samples can be seen in Figure 4.

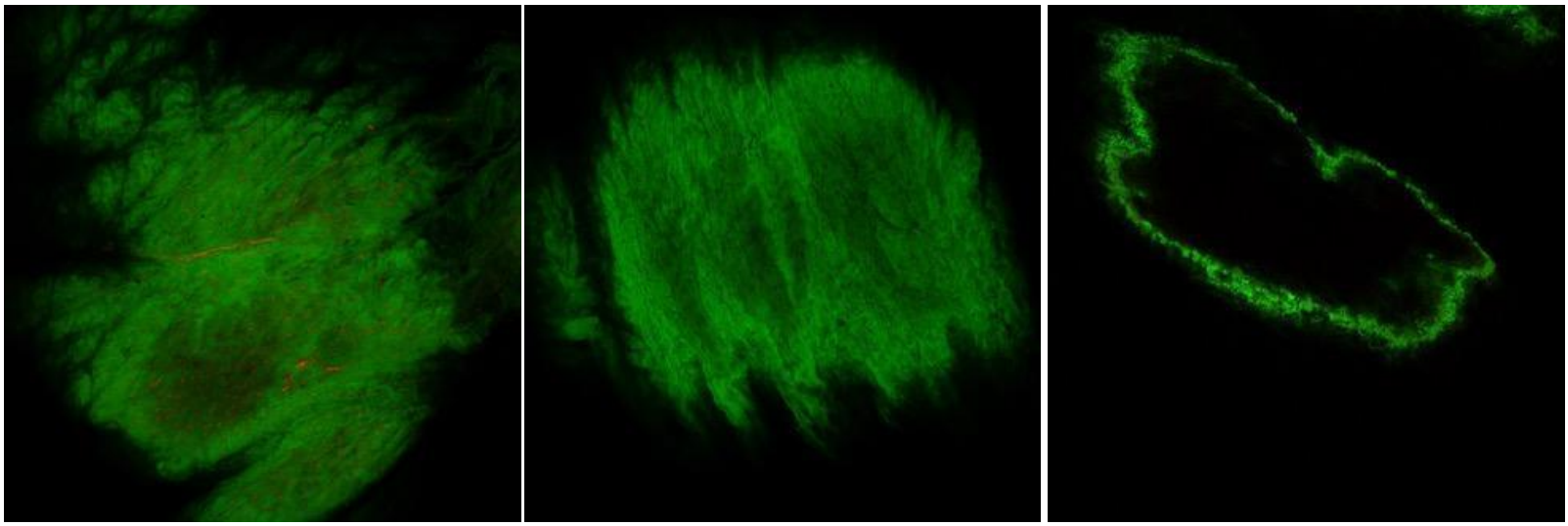

4A 4B 4C

Figure 4. Confocal images of the cleared twice (4A), cleared once group (4B), and uncleared groups (4C).

Discussion

As seen in Figure 4A, the UC group has an outline of green stained ECM and the red stained cells on the external areas of the sample are visible. The C1 group (Fig 4B) has a very clear cross section into the sample, however there are no visible red stained cells. The C2 group (Fig 4C) has clear staining of both the ECM and the cells. A potential reason the UC group did not have visibly stained cells is that during the clearing process the solution immersing the samples is frequently changed, and there may have been exposure to light that photobleached the stain during these solution changes. This likely did not occur in the C2 group, because the samples were exposed only to be imaged after staining. Overall, optical clearing of the sample greatly increases the imaging depth when using a confocal microscope. Clearing the samples twice proved to additionally increase the imaging depth. However, one challenge of clearing the samples twice, in this case, arose due to the nature of the stains. Staining was performed on the samples under aqueous conditions, meaning that the cleared samples had to be rehydrated and then dehydrated again to be re-cleared. This increased the length of time it took to complete the protocol. Utilizing an aqueous stain would render the dehydration steps associated with non-aqueous solutions unnecessary. A 3D reconstruction of the entire sample was not able to be completed due to working distance limitations of the confocal microscope available for this work.

For small samples in which the inner sections are most important, this protocol of staining, clearing, and imaging with a confocal microscope is highly useful. Due to the limited field of view and imaging depth associated with confocal microscopy, these practices may not be comprehensive enough. Additionally, imaging on a confocal microscope can be time consuming, taking at least 15 min. per image. Because confocal microscopy has these limitations, and the rodent knee samples of interest are relatively larger, SPIM methods are anticipated to be of greater use to image whole joints.

Whole Joint Imaging

Confocal imaging has limitations for use in the study of rodent models of osteoarthritis. The typical maximum imaging depth is 1000 microns, which is much smaller than the size of the average rat knee [15]. The field of view of confocal microscopes are also limited and may exclude portions of a larger sample, like a whole rodent joint [15]. It was useful, however, in establishing and testing a clearing and staining protocol. Another imaging technique that has greater promise in this field of study is selective plane illumination microscopy, or SPIM. SPIM is a form of microscopy that utilizes the same basic principle of optical scanning employed in confocal imaging. Advancements of SPIM over confocal microscopy include that only single plane is illuminated as each frame is captured, which decreases the amount of fluorophore bleaching and phototoxicity occurring during imaging, increasing viable imaging time, as well as improves specimen viability and high depth penetration [15]. Therefore, imaging with SPIM may allow for view of the entire joint and create a full 3D reconstruction of the joint. This application may allow for the evaluation of the entire joint space and the processing of the tissue may decrease the overall mechanical and chemical effects associated with traditional histology.

While SPIM devices are extremely useful, commercial units are often prohibitively expensive. To circumvent the prohibitive nature of the price tag of these devices, an open source platform was created to provide the necessary details to build a basic SPIM [19]. Currently, a SPIM is being created in the lab in order to have the capability to whole joint image at a low cost. With the intention of ultimately utilizing an OpenSPIM build for 3D histological assessment of rodent OA models, clearing and staining methods were applied to whole mouse knees and imaged on a Zeiss Lightsheet Z.1 SPIM to demonstrate feasibility of the imaging technique for larger musculoskeletal samples.

Methods

Mouse knee joints were used for initial studies with whole joint imaging, though our group hopes to scale these techniques to the rat, in the future. Naïve C57B16 male mice (n=5) were used in this study and the right and left knee joints were dissected and separately stored. The samples were fixed in formalin for 48 hours and then stored 70% EtOH. The left knee joints were then decalcified

with Cal-Ex at 4 °C for 36 hours. The clearing protocol used in this experiment was changed from the non-aqueous methyl salicylate protocol to an aqueous 2,2'-thiodiethanol (TDE) protocol. This was due to Zeiss SPIM sample chamber constraints.

The clearing protocol similarly involved sequential immersion of the samples in increasing concentrations of TDE in deionized water [17]. The samples were immersed for at least 12 hours at each concentration in 10% TDE, 25% TDE, 50% TDE, and finally 97% TDE. 97% TDE corresponds to a refractive index of 1.47 [17]. The optimal refractive index for bone is 1.55, thus the TDE solution alone is likely not to provide optimal refractive index matching as compared to methyl salicylate [17]. However, clearing was adequate for pilot imaging tests. After clearing, the samples were stained utilizing the same protocol as used for the porcine meniscus samples. The samples were then re-cleared using the same TDE protocol described.

Due to the lower refractive index of the TDE compared to the methyl salicylate (1.47 and 1.51, respectively), the tissue was not optimally clear. Because the bone marrow remained dark in the tissue, half of the samples were split and cleared of the bone marrow. Three right, non-decalcified joints were cut and two left, decalcified joints were cut. This is shown in Figure 5 below. Two whole joints were cut down and the muscle surrounding the joint was scraped away as much as possible. One joint was decalcified and one joint was not decalcified. They were imaged whole, then cut in half, and imaged again. The knee joints were imaged on the Zeiss Lightsheet Z.1.

	Right Knees	Left Knees
Total number of each	5	5
Decalcification	No	Yes
Number of samples cut	3	2

Figure 5. Table describing the samples used in this study.

Results

There did not seem to be an obvious difference in the clarity of the samples that were decalcified versus non-decalcified to the naked eye. These samples, however, did have a more gelatinous and soft texture as compared to the samples that were not de-calcified. Throughout the optical sections of the de-calcified samples, it qualitatively appeared that the details in the joint space structures were clearer. The decalcification process removes calcium deposits in the bone, and thus removes additional components that could cause light scattering. The samples that were cut prior to imaging, rather than after first being imaged whole, seemed to have clearer properties. This is likely due to the ability of the TDE to migrate into the center areas of the tissue for an extended period of time. One challenge of imaging on the SPIM arises from mounting orientation. It is worth noting that when the samples are tilted in relation to the focal plane, it is challenging to get a clear and focused view of the region of interest. While this detail is not inherently related to the specific sample preparations presented here, it will factor into sample preparations moving forward. Representative samples from each group are shown in Figure 6 below.

Figure 6. Images from the SPIM. Cut in half sample that was not decalcified (6A), cut in half sample that was decalcified (6B), whole sample that was not decalcified (6C), whole sample that was decalcified (6D), previously whole sample that was not decalcified (6E), previously whole sample that was decalcified (6F), 3D reconstruction image (6G), image of sample before laser excitation (6H).

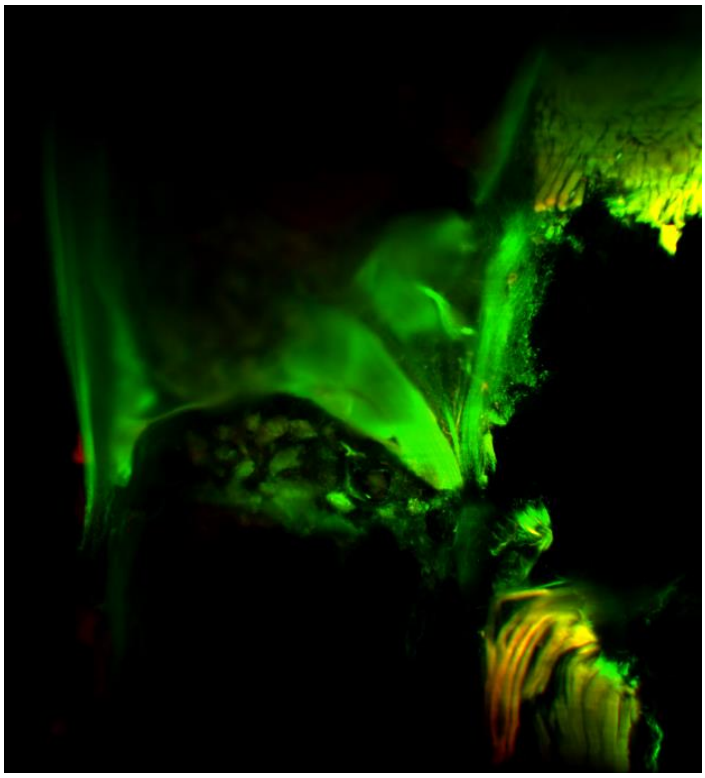

6A

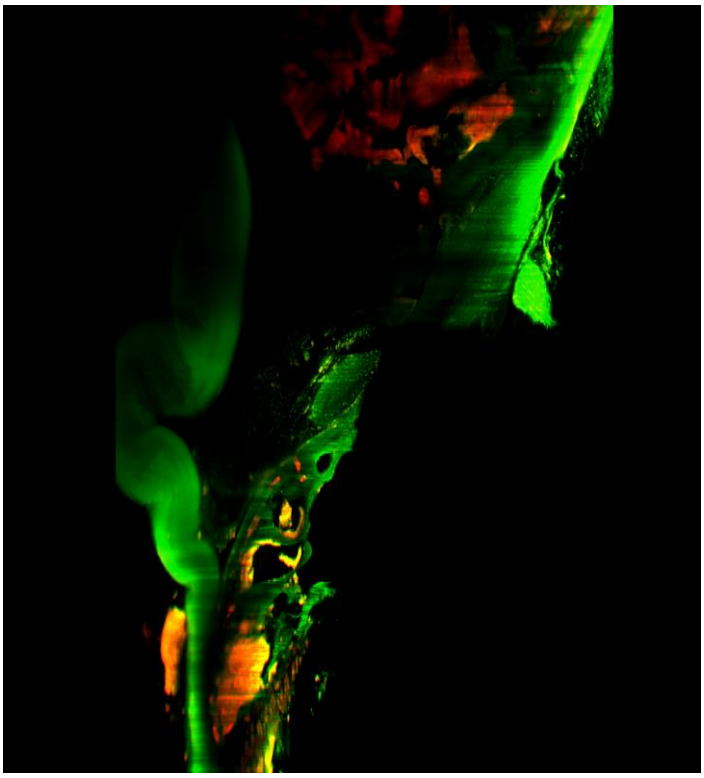

6B

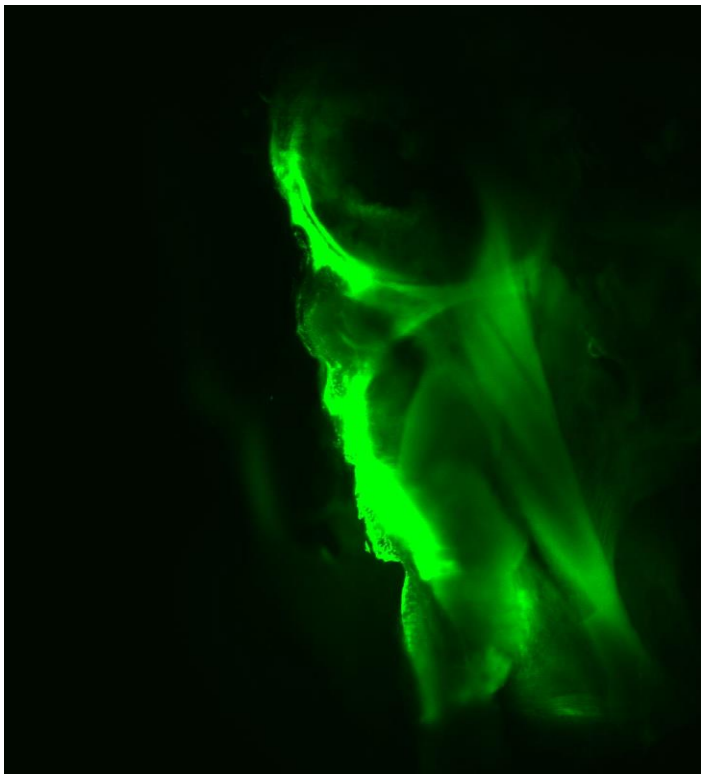

6C

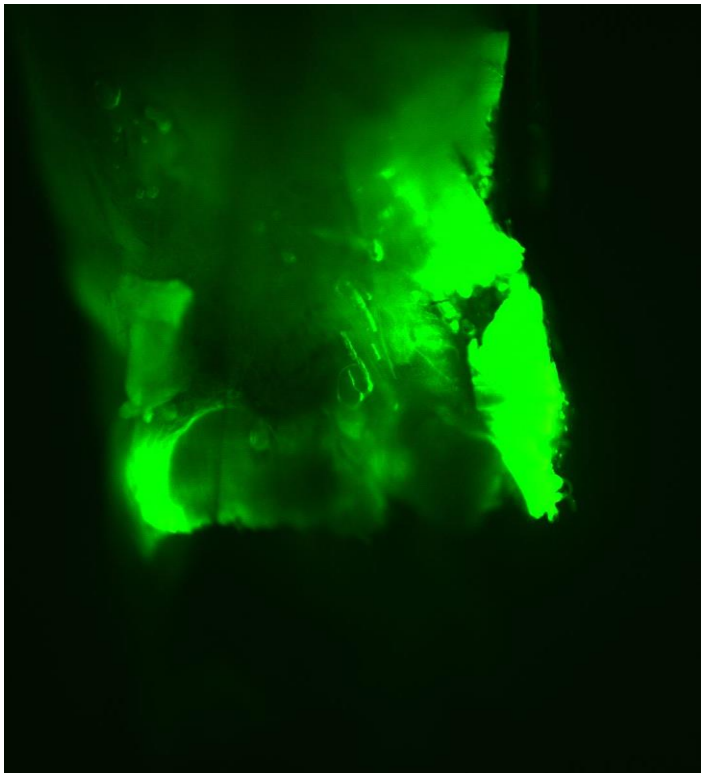

6D

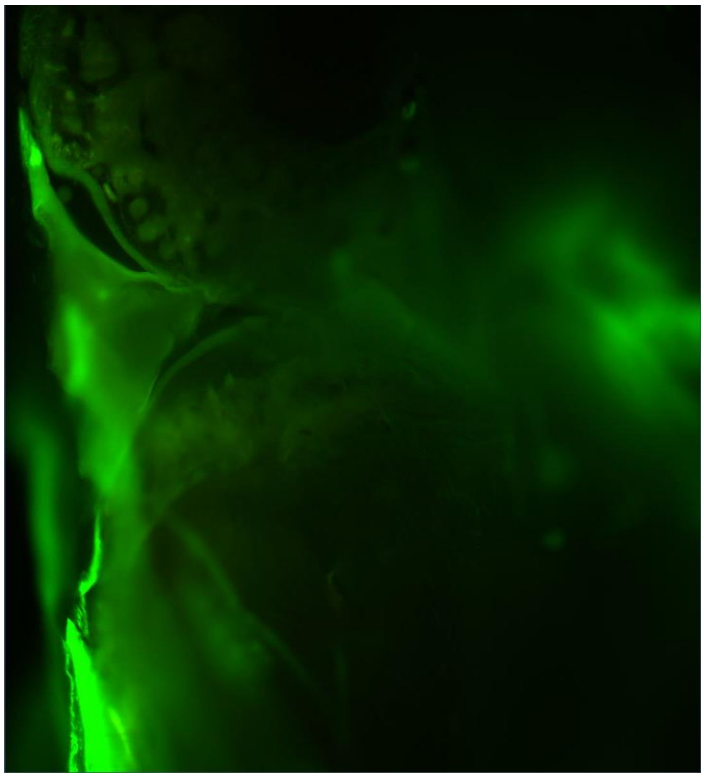

6E

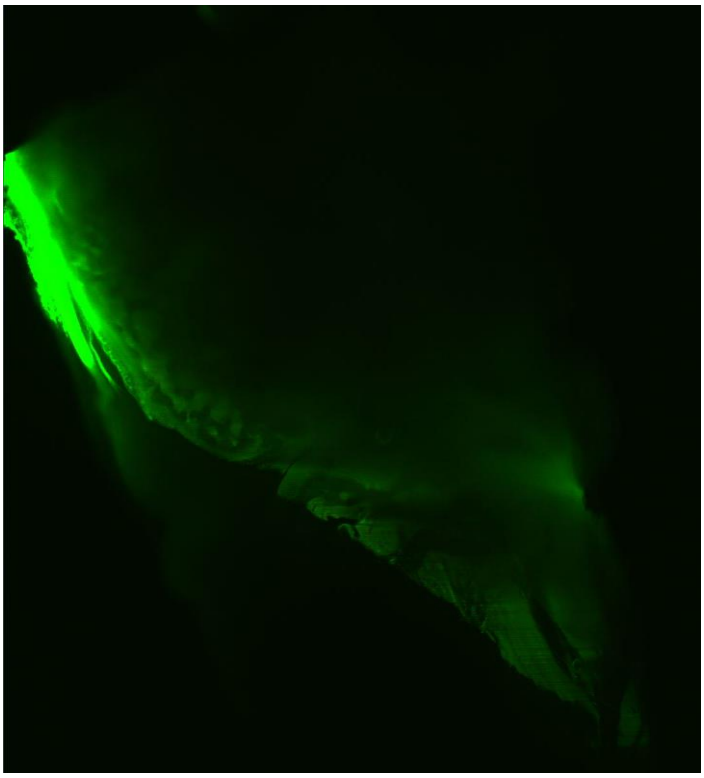

6F

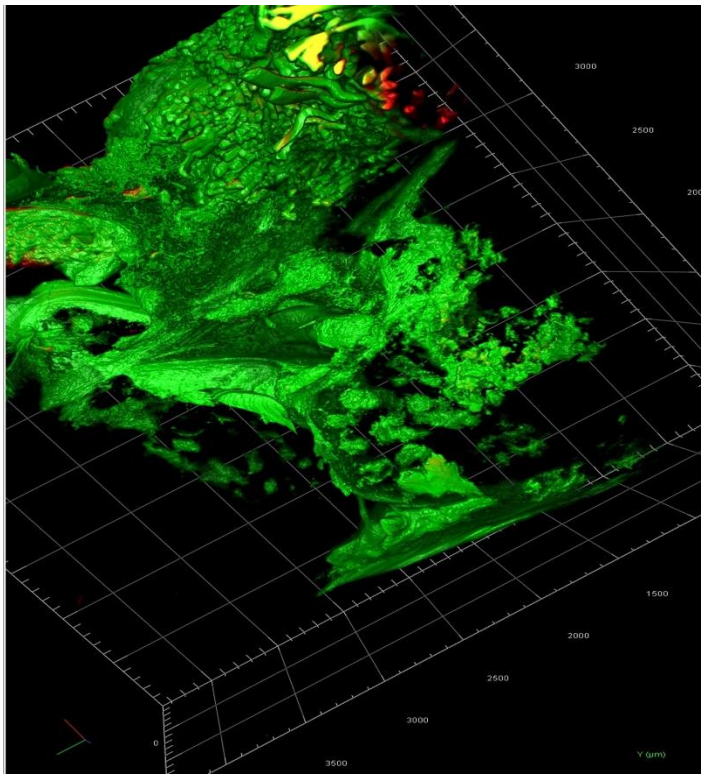

6G

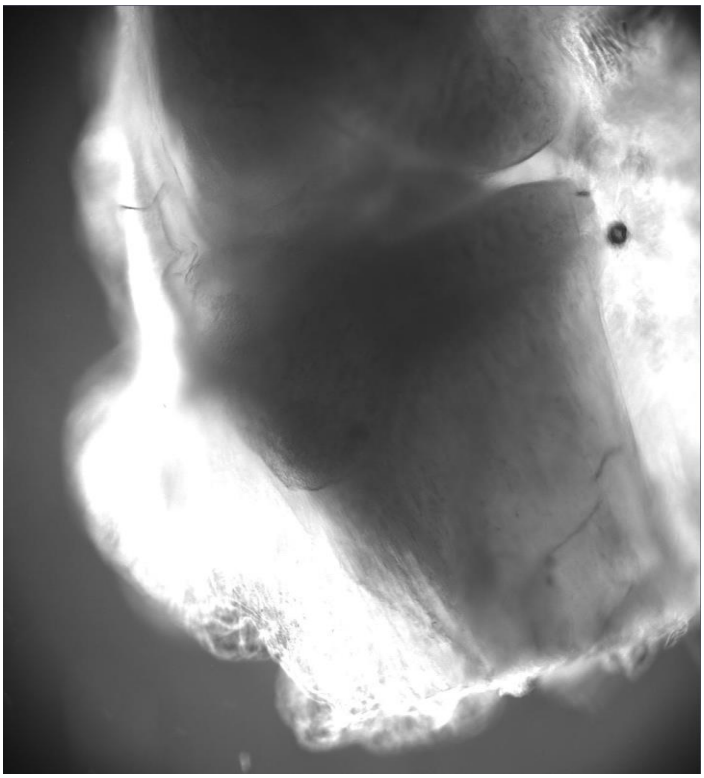

6H

Discussion

One key advantage of SPIM imaging over confocal microscopy is the imaging time per sample. A 500 microns thick sample can be imaged in under a minute at similar resolution to the confocal. For future studies, this will allow more data to be collected both faster and of greater depth as compared to confocal microscopy. Some challenges faced in this study arose from the clarity of the tissue. The lower refractive index of TDE compared to methyl salicylate impacted the quality of the images taken. As mentioned, the switch to TDE was due to the limitation of the SPIM used in this study, and is not intended as a permanent change with future work utilizing our groups own OpenSPIM build. It is possible to ensure an objective and sample chamber that are compatible with higher refractive index matching solutions, which will optimally allow for the use of methyl salicylate. The samples that were cut in half yielded more complete images, which is attributed primarily to poorer clearing of whole joint samples relative to halved samples. This is because the halved samples had a greater surface area exposed to the TDE that allowed for better penetration into the sample.

This study builds on the previous studies presented in this work and provides insight into how to further improve whole joint imaging in the future. With better clearing, this technique has promising utility in the OA space. The largest hindrance of this portion of the work was the opacity of the tissue. The smaller porcine meniscus samples described in the previous study were more easily penetrated by the clearing solutions. Additionally, whole joints have multiple tissue types with different refractive indices. This made the clearing portion of the procedure more challenging. The alignment of the tissue is something that should also be considered, moving forward, especially in cases where tissue is not optimally optically cleared, as the SPIM machine is nuanced and this specific condition provides an additional and avoidable challenge to getting to a good image. While the results of this pilot imaging study were not perfect, they provide valuable insight into how to further improve whole joint sample preparation specifically for SPIM applications. These improvements will increase the quality of the images taken, and provide data that will ultimately contribute to helping better assess the progression of OA in the joint over time.

Future Direction and Recommendations

As previously mentioned, histopathology provides valuable information about the changes that occur in the joint space in rodent models of OA. Improvements in histological techniques and available technology may ultimately contribute to more thorough assessments of these models and the progression of OA.

One improvement that may lend to improved consistency between studies and research groups is moving toward more detailed, fully quantitative measures of joint degeneration. For example, the use of GEKO, Guided User Interface for the Evaluation of Knee Osteoarthritis, which was software developed by the Allen lab, may to more consistent and faster grading. GEKO is a MATLAB based GUI that can be used as both a training and timesaving tool. It utilizes the parameters set by the Gerwin grading method, and allows the user to easily grade images by providing automated measurements based on user-identified points on an image. GEKO is one example of a tool that can be used to improve the consistency of grading histological joint images based on the Gerwin method. With the wider application of tools like GEKO, better field standardization of histological grading may be achieved, allowing for accurate and accessible comparisons across studies.

The first iteration of whole mouse joint SPIM imaging provides crucial information about how to improve and optimize the process. Sample preparation is key to producing high quality images that provide valuable histological data. In order to attempt whole joint imaging, a refractive index matching solution as close to the tissue of interest as possible (based on device limitations) should be used. The OpenSPIM build being created to further this work should incorporate design constraints specifically facilitating a refractive index that is close to the refractive index of the most opaque joint tissue, which is bone [17]. Because the bone marrow was not easily cleared or cleaned out of the samples, there was additional blockage of the laser which did not contribute to a high quality image. This may be avoided by using perfusing techniques to clear out the marrow. Perfusing with the index matching solution may also yield samples that are more optically clear and can be more easily imaged. The clearing of the samples may also be improved by agitation from a shaker plate.

When utilizing SPIM, samples should also be dissected to the point that the tissues being imaged are *only* the tissues of interest. For example, knee joints are surrounded by muscle tissue that provides support and stability to the joint. Thus, the muscle covers the areas surrounding the joint space. Because this muscle tissue is not of interest at the moment, it only serves to provide additional tissue that the laser light must penetrate. Cutting away this excess tissue as much as possible decreases additional light scattering due to the interfaces of multiple different tissues. With care, the samples should be stripped of all residual tissue that is not necessary to be imaged.

In this study, generalized stains for ECM and cell membrane were used to identify gross anatomical features and basic tissue structure. One disadvantage of the ECM stain is that it is excited at 488 nm. Many biological tissues, including cartilage and bone, autofluoresce at, or near, this wavelength. In order to determine whether the emission collected was due to the stain or autofluorescence, a non-stained sample could have been imaged at this same wavelength. This should be done for future studies that will use a 488 nm wavelength [20], [21]. For future studies, it may also be useful to target specific components of the joint space. For example, fluorescent labeling of collagen II or aggrecan can help track changes in the articular cartilage of the joint space over time.

This work provides valuable information about sample preparation and staining that will be used to better direct and optimize whole joint imaging. From this work, developing clearing and staining protocols with multiple clearing steps, the nuances of aqueous and non-aqueous optical clearing solutions, and certain sample preparations for whole joint imaging are now better understood for application in whole joint imaging.

References

[1] D. Felson, "Osteoarthritis: New Insights. Part 1: The Disease and Its Risk Factors", *Annals of Internal Medicine*, vol. 133, no. 8, p. 635, 2000.

[2] D. Felson, "Osteoarthritis: New Insights. Part 2: Treatment Approaches", *Annals of Internal Medicine*, vol. 133, no. 9, p. 726, 2000.

[3] E. Losina, E. Dervan, M. Daigle and J. Katz, "Studies of pain management in osteoarthritis: bedside to policy", *Osteoarthritis and Cartilage*, vol. 21, no. 9, pp. 1264-1271, 2013.

[4] M. Karsdal, C. Christiansen, C. Ladel, K. Henriksen, V. Kraus and A. Bay-Jensen, "Osteoarthritis – a case for personalized health care?", *Osteoarthritis and Cartilage*, vol. 22, no. 1, pp. 7-16, 2014.

[5] K. Lampropoulou-Adamidou, P. Lelovas, E. Karadimas, C. Liakou, I. Triantafillopoulos, I. Dontas and N. Papaioannou, "Useful animal models for the research of osteoarthritis", *European Journal of Orthopaedic Surgery & Traumatology*, vol. 24, no. 3, pp. 263-271, 2013.

[6] A. Bendele, "Animal models of osteoarthritis", *J Musculoskelet Neuronal Interact*, 2001.

[7] V. Kraus, F. Blanco, M. Englund, M. Karsdal and L. Lohmander, "Call for standardized definitions of osteoarthritis and risk stratification for clinical trials and clinical use", *Osteoarthritis and Cartilage*, vol. 23, no. 8, pp. 1233-1241, 2015.

[8] J. Martel-Pelletier, "Is osteoarthritis a disease involving only cartilage or other articular tissues?", *Eklem Hastalik Cerrahisi*, 2010.

[9] L. Creemers, M. Rutgers and D. Saris, "Evaluation of histological scoring systems for tissue-engineered, repaired and osteoarthritic cartilage", *Osteoarthritis and Cartilage*, vol. 18, no. 7, p. 1002, 2010.

[10] K. Pritzker, S. Gay, S. Jimenez, K. Ostergaard, J. Pelletier, P. Revell, D. Salter and W. van den Berg, "Osteoarthritis cartilage histopathology: grading and staging", *Osteoarthritis and Cartilage*, vol. 14, no. 1, pp. 13-29, 2006.

[11] N. Gerwin, A. Bendele, S. Glasson and C. Carlson, "The OARSI histopathology initiative – recommendations for histological assessments of osteoarthritis in the rat", *Osteoarthritis and Cartilage*, vol. 18, pp. S24-S34, 2010.

[12] S. Chatterjee, "Artefacts in histopathology", *Journal of Oral and Maxillofacial Pathology*, vol. 18, no. 4, p. 111, 2014.

[13] K. Ostergaard, J. Petersen, C. Andersen, K. Bendtzen and D. Salter, "Histologic/histochemical grading system for osteoarthritic articular cartilage. Reproducibility and validity", *Arthritis & Rheumatism*, vol. 40, no. 10, pp. 1766-1771, 1997.

[14] D. Richardson and J. Lichtman, "Clarifying Tissue Clearing", *Cell*, vol. 162, no. 2, pp. 246-257, 2015.

[15] "Confocal Microscope", *Cas.miamioh.edu*. [Online]. Available: https://www.cas.miamioh.edu/mbiws/microscopes/confocal.html. [Accessed: 28- Mar- 2018].
[16] J. Huisken and D. Stainier, "Selective plane illumination microscopy techniques in developmental biology", *Development*, vol. 136, no. 12, pp. 1963-1975, 2009.
[17] I. Berke, J. Miola, M. David, M. Smith and C. Price, "Seeing through Musculoskeletal Tissues: Improving In Situ Imaging of Bone and the Lacunar Canalicular System through Optical Clearing", *PLOS ONE*, vol. 11, no. 3, p. e0150268, 2016.
[18] M. Upton, C. Gilchrist, F. Guilak and L. Setton, "Transfer of Macroscale Tissue Strain to Microscale Cell Regions in the Deformed Meniscus", *Biophysical Journal*, vol. 95, no. 4, pp. 2116-2124, 2008.
[19]"OpenSPIM", *Openspim.org*. [Online]. Available: http://openspim.org/Welcome_to_the_OpenSPIM_Wiki. [Accessed: 28- Mar- 2018].
[20] F. Stelzle, C. Knipfer, W. Adler, M. Rohde, N. Oetter, E. Nkenke, M. Schmidt and K. Tangermann-Gerk, "Tissue Discrimination by Uncorrected Autofluorescence Spectra: A Proof-of-Principle Study for Tissue-Specific Laser Surgery", *Sensors*, vol. 13, no. 10, pp. 13717-13731, 2013.
[21] V. Tuchin, "Optical clearing of tissues and blood using the immersion method", *Journal of Physics D: Applied Physics*, vol. 38, no. 15, pp. 2497-2518, 2005.